Eur. Phys. J. D (2017) 71: 249
DOI: 10.1140/epjd/e2017-80247-x

THE EUROPEAN PHYSICAL JOURNAL D

Regular Article

Quantum sensing of rotation velocity based on transverse field Ising model

Yu-Han Ma[1,2] and Chang-Pu Sun[1,2,a]

[1] Beijing Computational Science Research Center, Beijing 100193, P.R. China
[2] Graduate School of Chinese Academy of Engineering Physics, Beijing 100084, P.R. China

Received 11 April 2017 / Received in final form 23 June 2017
Published online 10 October 2017 –

Abstract. We study a transverse-field Ising model (TFIM) in a rotational reference frame. We find that the effective Hamiltonian of the TFIM of this system depends on the system's rotation velocity. Since the rotation contributes an additional transverse field, the dynamics of TFIM sensitively responses to the rotation velocity at the critical point of quantum phase transition. This observation means that the TFIM can be used for quantum sensing of rotation velocity that can sensitively detect rotation velocity of the total system at the critical point. It is found that the resolution of the quantum sensing scheme we proposed is characterized by the half-width of Loschmidt echo of the dynamics of TFIM when it couples to a quantum system S. And the resolution of this quantum sensing scheme is proportional to the coupling strength δ between the quantum system S and the TFIM, and to the square root of the number of spins N belonging the TFIM.

1 Introduction

Quantum sensing is a kind of sensing scheme, which utilizes the quantum effects to enhance the measurement accuracy. Quantum gyroscope [1] is a kind of quantum sensor which makes use of quantum sensing schemes for rotation velocity measurement. For example, atom interferometer gyroscope (AIG) makes use of the interference of matter waves, and was first achieved in experiment in 1991 [2]. Another quantum gyroscope is nuclear magnetic resonance gyroscope (NMRG), which detects the rotation velocity by detecting the precession frequency of the nuclear magnetic moment in the non-inertial system [3]. In recent years, a K-3He-based NMRG has been experimentally verified that the resolution of such gyroscopes is between 0.01°/h and 0.1°/h [4]. In reference [5], information on the NMRG under development by Northrop Grumman Corporation is given, specifically illustrating the different structures of NMRGs of different phases. In order to facilitate the application, the miniaturization of NMRG is also a matter of great concern. The structure, performance and parameters of the micro-NMRG are reported in [6]. Both AIG and NMRG are quantum gyroscopes with high accuracy in measurement, and are used in high precision inertial navigation and military strategic system.

For a future quantum sensing scheme with much higher accuracy, we need to explore the roles which could be positive or negative of new quantum effects. The key to the quantum sensing scheme is the measurement accuracy, or in our case, the resolution for rotation velocity, which is physically reflected by the response of its dynamics to the rotation velocity of the system. In this paper, we study the dynamics of transverse field Ising model (TFIM) and found the Loschmidt echo (LE) of TFIM is sensitive to the rotation velocity at the critical point of quantum phase transition (QPT). In 2006, Quan et al. [7] found that when a TFIM couples with a quantum system S, and is turned into critical point of QPT, the quantum decoherence phenomena of system S will be significantly enhanced, which is characterized by the rapid decay of LE of the dynamics of TFIM around the critical point. For TFIM in non-inertial reference frame, its QPT behavior depends on the rotation velocity Ω of the total system sensitively as the Ω behaves as an external transverse field.

The QPT of TFIM in rotational reference frame will be affected directly by the rotation velocity of the system, therefore it is feasible to achieve the measurement of rotation velocity through recording the QPT of TFIM. With this consideration, we designed a quantum sensing scheme to carry out rotation velocity measurements by detecting the QPT of TFIM in non-inertial reference frame. This paper is arranged as follows. In Section 2, we study the Hamiltonian of the TFIM in non-inertial system and thus examine the response of the TFIM's LE to the rotation velocity Ω of the system. In Section 3, we propose a

[a] e-mail: cpsun@csrc.ac.cn

quantum sensing scheme based on TFIM in rotational reference frame, and give its resolution for rotation velocity Ω. Conclusion of our results are given in Section 4.

2 Transverse field Ising model in non-inertial reference frame

In this section we consider a coupled spin system with an external field in a rotational reference frame. The Hamiltonian of the TFIM in the stationary system reads

$$H_0 = -J\sum_i \left(\sigma_i^z\sigma_{i+1}^z + \lambda\sigma_i^x\right), \tag{1}$$

where J and λ characterize the strengths of the inter-spin interaction and the coupling to the transverse field, $\sigma_i^\alpha\ (\alpha \in \{x, y, z\})$ are Pauli operators defined in the state space of the ith particle. Note that, the critical point for QPT of TFIM is $\lambda_c = 1$ [7,8], below which the TFIM will generate spontaneous magnetization. As shown in Figure 2, while a spin chain of TFIM is placed in a rotating system which rotates with an angle $\theta(t)$ relative to the stationary reference frame, the time-dependent Hamiltonian of TFIM is

$$H(t) = -J\sum_i \left(\sigma_i^z(t)\,\sigma_{i+1}^z(t) + \lambda\sigma_i^x(t)\right), \tag{2}$$

where $\sigma_i^\alpha(t)$ are Pauli matrices in the coordinate system which is relatively stationary with the TFIM. With the help of rotation matrix $D_{\vec{n}}(\theta)$, $\sigma_i^\alpha(t)$ can be explicitly expressed by σ_i^α

$$\begin{pmatrix} \sigma_i^x(t) \\ \sigma_i^y(t) \\ \sigma_i^z(t) \end{pmatrix} = D_{\vec{n}}(\theta) \begin{pmatrix} \sigma_i^x \\ \sigma_i^y \\ \sigma_i^z \end{pmatrix}, \tag{3}$$

where $\vec{n}$ is the direction vector of the rotation axis. When the system rotates counterclockwise in the x-direction, the rotation matrix is

$$D_x(\theta) = \begin{pmatrix} 1 & 0 & 0 \\ 0 & \cos\theta & -\sin\theta \\ 0 & \sin\theta & \cos\theta \end{pmatrix}. \tag{4}$$

In addition, we set $\theta(0) = 0$, so that $H(0) = H_0$.

The Schrodinger's equation in the rest reference frame for TFIM with rotation angle $\theta(t)$ is $i\hbar\partial\Psi/(\partial t) = H(\theta)\Psi$, where Ψ is the wave function of TFIM in the rest reference frame. Obviously, $\Psi' = R(\theta)\Psi$ represents the wave function of TFIM in the rotation reference frame, where $R(\theta) = \exp\left(-i\vec{\theta}\cdot\vec{S}/\hbar\right)$ is the rotation operator and $\vec{S} = \sum_i \vec{s_i}$ is the total spin of the TFIM, while $\vec{s_i}$ is the spin of the ith particle. Thus the Schrodinger's equation for Ψ' is

$$i\hbar\frac{\partial}{\partial t}\Psi' = \left(R(\theta)\,H(t)\,R^\dagger(\theta) - i\hbar R(\theta)\frac{\partial}{\partial t}R^\dagger(\theta)\right)\Psi'. \tag{5}$$

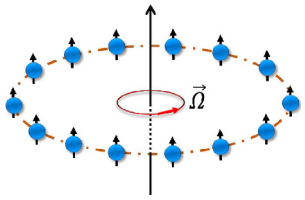

Fig. 1. Transverse field Ising model in rotation reference frame. The whole system is rotating around the axis with rotation velocity $\vec{\Omega}$.

Equation (5) indicates the effective Hamiltonian of the rotating TFIM in non-inertial reference is

$$H_{eff} = R(\theta)\,H(t)\,R^\dagger(\theta) - i\hbar R(\theta)\frac{\partial}{\partial t}R^\dagger(\theta). \tag{6}$$

For the system rotating around x axis, $R(\theta)$ is

$$R_x(\theta) = \exp\left(-i\theta\sum_i \sigma_i^x/2\right). \tag{7}$$

It follows from equations (2)–(4), (6) and (7) that the effective Hamiltonian for the rotating TFIM in non-inertial reference frame is obtained as

$$H_{eff} = -J\sum_i \left[\sigma_i^z\sigma_{i+1}^z + \left(\lambda - \frac{\hbar\Omega}{2J}\right)\sigma_i^x\right]. \tag{8}$$

Here $\Omega = d\theta/(dt)$ indicates the instantaneous rotation velocity of the total system. It is imagined from equation (1) that the rotation term in equation (8) can be regarded as an effective magnetic field interacting with spins in the x direction. For a single spin in TFIM, if we ignore the interaction with other spins, the effective Hamiltonian will be $H_{eff}^i = -J\left[\lambda - \hbar\Omega/(2J)\right]\sigma_i^x$, which is the same as that of the nuclear magnetic resonance (NMR). The physical meaning of this rotation term is similar to the Coriolis force, which is known as a basic non-inertial effect in classical mechanics (Fig. 1).

In 2006, Quan et al. [7] pointed out that, when TFIM couples with a two level quantum system S, the decoherence of S will be effectively enhanced while the TFIM is at its critical point for QPT. This phenomenon was proved to be directly related to the Loschmidt echo (LE) of the dynamical behavior of TFIM and has been observed experimentally [9,10]. The Hamiltonian they used to describe the interaction between S and TFIM is

$$H(\lambda, \delta) = -J\sum_i \left(\sigma_i^z\sigma_{i+1}^z + \lambda\sigma_i^x + \delta\,|e\rangle\langle e|\,\sigma_i^x\right), \tag{9}$$

where J,λ,$\sigma_i^\alpha\ (\alpha \in \{x, y, z\})$ are consistent with our previous explanation, and δ is the coupling strength between TFIM and quantum system S. If the whole system is placed in a rotating system, there will be a correction to

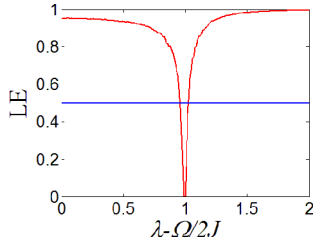

Fig. 2. Loschmidt echo as a function of rotation velocity Ω for system with $N = 2000$, $\delta = 0.01$. This figure shows that around the critical point $\widetilde{\lambda} = 1$, a tiny change of Ω will cause rapid change of LE. The blue line in the figure marks $L = 0.5$, and the length of which inside the valley of LE represent the half-width of LE. The half-width of LE demonstrates the resolution of LE to the change of rotation velocity and will be further discussed in Section 4.

Hamiltonian in equation (9), which is

$$H(\widetilde{\lambda}, \delta) = -J \sum_i (\sigma_i^z \sigma_{i+1}^z + \widetilde{\lambda} \sigma_i^x + \delta \left|e\right\rangle \left\langle e\right| \sigma_i^x). \quad (10)$$

Here,

$$\widetilde{\lambda} \equiv \lambda - \frac{\hbar \Omega}{2J}, \quad (11)$$

is defined as the total effective magnetic field which is modified by the rotation velocity Ω of the non-inertial reference frame. To show the effect of the rotation on the dynamic of the system, we calculate the LE of TFIM [7] by taking $N = 2000$, $\delta = 0.01$, $\lambda = 2$, $\hbar = 1$, $\Omega \in [0, 4J]$. The result we get is demonstrated in Figure 2, which shows the relationship between LE and the effective magnetic field $\widetilde{\lambda}$.

It is obvious in Figure 2 that a slight change of rotation velocity around the critical point for QFT of TFIM $\widetilde{\lambda} = 1$ results in a significant change in the value of LE, which indicates that the dynamics of TFIM is sensitive to the rotation velocity at the critical point of QPT. This suggests that TFIM can serve as a gyroscope in principle to measure the rotation velocity of a non-inertial system.

3 Quantum sensing scheme for rotation velocity

Due to the sensitive dependence of the parameters (λ, Ω) to QPT of TFIM, there comes an idea that the rotation of a system can be detected through the observation of TFIM's QPT. In another word, we propose a quantum sensing scheme which makes use of the quantum phase transition effect of TFIM. It can be seen in Figure 2 that the significant response of LE to the change of rotation velocity occurs only near the critical point for QPT of TFIM.

To utilize the QPT effect to detect the rotation velocity sensitively, we need to keep $\widetilde{\lambda}$ near the critical point $\lambda_c = 1$. But for any rotation velocity to be measured, $\widetilde{\lambda}$ may be far away from λ_c, thus we need to adjust the magnetic field λ to ensure that $\widetilde{\lambda}$ fall in the range we are expecting. For the sensing scheme to be working properly, we need the magnetic field to be adjusted into the vicinity area of $\widetilde{\lambda}$, but the problem is we do not know the value of $\widetilde{\lambda}$ in advance. To solve this problem, we present the following measurement scheme, which is illustrated in Figure 3.

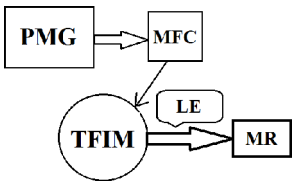

Fig. 3. Workflow of the quantum sensing scheme. The entire quantum sensing scheme needs to be achieved by the following modules. A pre-measuring gyroscope (PMG), which may be the Micro-Electro-Mechanical System gyroscope or a fiber optic gyroscope or other kinds of classical gyroscopes, a magnetic filed controller (MFC), a transverse field Ising model (TFIM) and circuitry to connect the entire system.

First, we use a pre-measuring gyroscope (PMG) to carry out a pre-measurement and send the result Ω_0 to the magnetic filed controller (MFC). Then the MFC will adjust the amplitude of the magnetic filed inside the module of TFIM to make the effective magnetic field $\widetilde{\lambda}$ in the vicinity of the critical point that $\widetilde{\lambda} \approx \lambda_c = 1$. In addition, the sensitivity of the LE of the TFIM near the critical point of QPT has been experimentally observed [9,10]. This illustrates the feasibility of implementing the TFIM module in experiment. For example, in reference [9], the authors use a NMR system to simulate the Hamiltonian of TFIM. In view of the fact that the nitrogen-vacancy (NV) color center has a long coherence time [11,12], we also hope that the TFIM module can be realized by using a plurality of interacting NV color centers. Let σ be the resolution of PMG, then the rotation velocity to be measured is in the following range

$$\Omega_1 \in [\Omega_0 - \sigma, \Omega_0 + \sigma]. \quad (12)$$

From equations (11) and (12), we obtain the magnetic field adjustment range of MFC

$$1 + \frac{\hbar}{2J}(\Omega_0 - \sigma) \leq \lambda \leq 1 + \frac{\hbar}{2J}(\Omega_0 + \sigma), \quad (13)$$

which is the key to make $\widetilde{\lambda}$ change in the vicinity of TFIM's critical point. When the QPT of TFIM occurs at $\widetilde{\lambda} = \lambda_c = 1$, the LE will rapidly decay to zero. At the same time, the amplitude of the magnetic field is denoted as $\lambda = \lambda_0$. Thus the rotation velocity is measured as a result that

$$\Omega_1 = \frac{2J}{\hbar}(\lambda_0 - 1). \quad (14)$$

However, if we want to use this quantum sensing scheme to achieve a meaningful measurement for rotation velocity(the resolution is improved by TFIM compared with that of PMG, the distinguish-ability of TFIM's QPT to rotation velocity should be higher than that of PMR, which is to say

$$\triangle\Omega < \sigma, \tag{15}$$

where $\triangle\Omega$ is the resolution of TFIM's QPT to rotation velocity. For a quantum sensing scheme, its resolution is an important parameter, which indicates the minimum rotation velocity it can measure. In the above scheme we have proposed, the resolution of TFIM's QPT to rotation velocity is characterized by the half-width of LE of the dynamics of TFIM. The smaller the LE's half-width is, the smaller rotation velocity the system can discern, and thus the higher resolution the system processes. The exact expression for LE of the system with Hamiltonian in equation (9) was given in paper [7]. It can be seen from equation (10) that, while the entire system is placed in non-inertial reference frame, the Hamiltonian has the same form as in equation (9), except λ is replaced by $\widetilde{\lambda}$. By using the constant variable method, we make the replacement $\lambda \to \widetilde{\lambda}$ for the solutions given in paper [4]. Thus the exact expression for $L(\widetilde{\lambda},t)$ is naturally obtained as

$$L(\widetilde{\lambda},t) = \prod_{k>0}[1 - \sin^2(2\alpha_{\widetilde{\lambda},k})\sin^2(\varepsilon_e^{\widetilde{\lambda},k}t)], \tag{16}$$

where

$$\alpha_{\widetilde{\lambda},k} = \frac{1}{2}[\theta_{\widetilde{\lambda},k}(0) - \theta_{\widetilde{\lambda},k}(\delta)],$$

and

$$\theta_{\widetilde{\lambda},k}(\delta) = \arctan\{-\sin(ka)/[\cos(ka) - (\widetilde{\lambda}+\delta)]\},$$

and the single quasiexciation energy [13]

$$\varepsilon_e^{\widetilde{\lambda},k}(\delta) = 2J\sqrt{1 + (\widetilde{\lambda}+\delta)^2 - 2(\widetilde{\lambda}+\delta)\cos(ka)}.$$

Here, the Bloch wave vector k takes the discrete values $2n\pi/(Na)$ $(n = 1, 2, \ldots, N/2)$, where a and N are the lattice spacing and particle number of TFIM. We first make an analytical analysis by considering the partial sum with a cutoff wave vector K_c, thus

$$S(\widetilde{\lambda},t) = \ln L_c = -\sum_{k>0}^{K_c}\left|\ln F_k(\widetilde{\lambda},t)\right|, \tag{17}$$

where $F_k(\widetilde{\lambda},t) = 1 - \sin^2(2\alpha_{\widetilde{\lambda},k})\sin^2(\varepsilon_e^{\widetilde{\lambda},k}t)$, and K_c can be expressed by a cutoff number N_c as $K_c = N_c\pi/(Na)$.

When $K_c a \ll 1$ $(N_c \ll N)$

$$S = -\frac{\delta^2 m\sin^2[2J(1-\widetilde{\lambda})t/\hbar]}{(1-\widetilde{\lambda})^2(1-\widetilde{\lambda}-\delta)^2}, \tag{18}$$

where

$$m \equiv \frac{4\pi^2 N_c(N_c+1)(2N_c+1)}{6N^2}. \tag{19}$$

It follows from equations (17) and (18) that

$$L_c = \exp\left\{-\frac{\delta^2 m\sin^2[2J(1-\widetilde{\lambda})t/\hbar]}{(1-\widetilde{\lambda})^2(1-\widetilde{\lambda}-\delta)^2}\right\}. \tag{20}$$

Around the critical point for QPT, we set $\epsilon = 1 - \widetilde{\lambda} - \delta$, as a result, if $2J(\epsilon+\delta)t/\hbar \ll 1$ we have

$$L_c(\epsilon,t) = e^{-4\frac{\delta^2}{\epsilon^2}mJ^2t^2/\hbar^2}. \tag{21}$$

To get the time-independent half-width of L_c, we define the characteristic time $t_0 \equiv \hbar/2J$, and then we can calculate the half-width of L_c, which is defined as ϵ_0, at $t = t_0$

$$\frac{1}{2} = L_c(\epsilon_0, t_0) = e^{-\delta^2 m/\epsilon_0^2}. \tag{22}$$

In this case, the half-width of L_c is obtained as

$$\epsilon_0 = \delta\sqrt{m}/\sqrt{\ln 2} \approx \delta\sqrt{m}. \tag{23}$$

For the above analytical calculation, we further assume that the momentum cutoff K_c is an N-independent constant in the limit $N \to \infty$, i.e., we have

$$N_c = \alpha N, \tag{24}$$

where $\alpha = K_c a/\pi$ is also an N-independent constant. Later we will verify this assumption and determine the value of α via exact numerical calculation. Using relation (24), we find that the parameter m defined in equation (19) is expressed as

$$m = \frac{4\pi^2\alpha N(\alpha N+1)(2\alpha N+1)}{6N^2} \approx \frac{4}{3}\pi^2\alpha^3 N \equiv \eta N. \tag{25}$$

Thus, equation (25) of the half-width ϵ_0 of L_c becomes

$$\epsilon_0 \approx \delta\sqrt{m} = \sqrt{\eta}\delta N^{\frac{1}{2}}. \tag{26}$$

Notice that $\eta = 4\pi^2\alpha^3/3$ is an N-independent parameter.

Equation (26) implies that the half-width ϵ_0 or the behavior of L_c as a function of $\tilde{\lambda}$ is determined by $\delta N^{\frac{1}{2}}$. This conclusion can be justified by numerical calculation by taking $\lambda = 2$, $\hbar = 1$, $\Omega \in [0, 4J]$, and the results are shown in Figure 4, in which we illustrate L_c for the cases

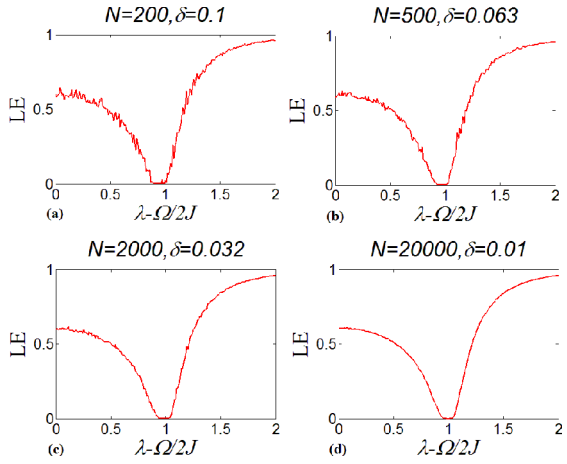

Fig. 4. Diagrams of Loschmidt echo as a function of rotation velocity Ω in the case where $\sqrt{N}\delta = \sqrt{2}$. (a) System with $N = 200$ and $\delta = 0.1$. (b) System with $N = 500$ and $\delta = 0.063$. (c) System with $N = 2000$ and $\delta = 0.032$. (d) System with $N = 20\,000$ and $\delta = 0.01$. These curves of LE have the similar configuration.

where the parameter $\delta N^{\frac{1}{2}}$ is fixed at $\sqrt{2}$ while N takes different values at 200, 500, 2000, and 20 000. It is clearly shown that in these cases the behavior of L_c are quite similar. In Figure 5 we show L_c for the cases with fixed value of N and different values of δ. The calculation shows that the width of L_c decrease significantly with δ. The numerical results in the two figures clearly confirm the results given by our analytical analysis, i.e., the behavior of L_c is determined by the parameter $\delta N^{\frac{1}{2}}$ in the large-N limit. Furthermore, with the help of equation (26) and the exact numerical solution of ϵ_0 given by equation (16), we fit the value of parameter α or η for system with $N = 20\,000$. As shown in Figure 6 , the fitting gives $\sqrt{\eta} = 0.375$. According to equations (11) and (26), the resolution of our sensing scheme is obtained as

$$\triangle\Omega = \frac{2J\epsilon_0}{\hbar} = 2\sqrt{\eta}\omega_0\delta\sqrt{N} = 0.75\omega_0\delta\sqrt{N}, \qquad (27)$$

where $\omega_0 \equiv J/\hbar$ is the characteristic coupling frequency of the spins' interaction. As a theoretical result, the resolution given in equation (27) does not have the upper bound in principle. However, the experimental achievable resolution depends on the optimal implementation of several parameters that affect the resolution in a particular experimental system. For $\omega_0 \sim 1\,\mathrm{Hz}$, $\delta = 1 \times 10^{-5}$, $N = 2000$, $\triangle\Omega \approx 3.4 \times 10^{-4\circ}/\mathrm{s}$, which is close to the resolution of Ring Laser Gyroscope, Interferometric Fiber Optic Gyroscope, and Resonant Fiber Optic Gyroscope [14]. In another case, when $\omega_0 \sim 0.01\,\mathrm{Hz}$, $\delta = 1 \times 10^{-6}$, $N = 100$, the resolution $\triangle\Omega \approx 7.5 \times 10^{-8\circ}/\mathrm{s}$. This achieves the resolution range of the AIG [15]. With the help of equation (15), the constraint condition (15) becomes

$$\delta\sqrt{N} < 1.33\frac{\sigma}{\omega_0}. \qquad (28)$$

Here, σ is the resolution of the PMG.

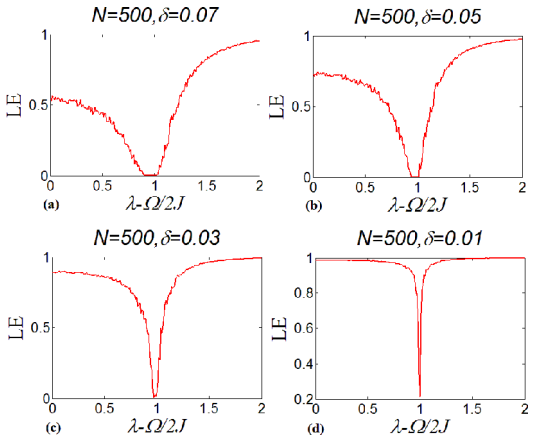

Fig. 5. Diagrams of Loschmidt echo as a function of rotation velocity Ω for system with $N = 500$, and δ respectively take $0.07, 0.05, 0.03, 0.01$ in (a), (b), (c) and (d). These diagrams show that the valley of the curve become narrower when δ is decreasing.

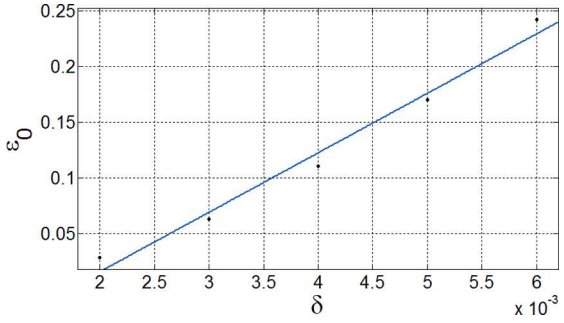

Fig. 6. Half-width of Loschmidt echo changes with different δ. The black points in this figure is LE's half-width ϵ_0 given by numerical calculation, and the blue line is the fitting line of these points. It is obviously there exist a liner relationship between ϵ_0 and δ, and the proportionality coefficient is given as $\sqrt{\eta} = 0.375$.

4 Conclusion

In summary, we have studied the rotation effect of the reference frame on the QPT of the transverse field Ising model (TFIM). Since the rotation velocity will apply an equivalent magnetic field to the original transverse field, the dynamic evolution of the TFIM is sensitive to the rotation velocity of the reference frame at the critical point of TFIM; when we adjust the original transverse field to the vicinity of the critical point for QPT of TFIM, the Loschmidt echo will change significantly due to small changes of rotation velocity. This finding inspire us to design a quantum sensing scheme for measuring rotation velocity.

The quantum sensing scheme presented in this paper is composed of three steps. First, the approximate range of the rotation velocity is obtained by the pre-measurement. Then the magnetic field is adjusted based on the result of pre-measurement to tune the TFIM near the critical point of QPT. Finally, the rotation velocity of the system

is obtained by analyzing the feature of LE. Furthermore, we found the resolution of this quantum sensing scheme is proportional to $\delta\sqrt{N}$, where δ is the coupling strength between quantum system S and TFIM, and N is the number of spins belongs to TFIM.

Y.H. Ma would like to thank Jin-fu Chen, Yi-nan Fang, Guo-hui Dong and Xin Wang in Beijing Computational Science Research Center for helpful discussion. This study is supported by the National Basic Research Program of China (Grant Nos. 2014CB921403 & 2016YFA0301201), the NSFC (Grant Nos. 11421063 & 11534002), and the NSAF (Grant No. U1530401).

Author contribution statement

Yu-Han Ma proposed the idea and wrote the manuscript, Chang-Pu Sun provided constructive discussions and revised the manuscript.

References

1. M.N. Armenise, C. Ciminelli, F. Dell'Olio et al., *Advances in gyroscope technologies [M]* (Springer Science & Business Media, Berlin Heidelberg, 2010)
2. B. Barrett, R. Geiger, I. Dutta et al., C. R. Phys. **15**, 875 (2014)
3. T.G. Walker, M.S. Larsen, Adv. At. Mol. Opt. Phys. **65**, 373 (2016)
4. T.W. Kornack, R.K. Ghosh, M.V. Romalis, Phys. Rev. Lett. **95**, 230801 (2005)
5. M. Larsen, M. Bulatowicz, in *IEEE International, Frequency Control Symposium (FCS)* (IEEE, 2012), p. 1
6. R.M. Noor, V. Gundeti, A.M. Shkel, in *IEEE International Symposium on Inertial Sensors and Systems (INERTIAL)* (IEEE, 2017), p. 156
7. H.T. Quan, Z. Song, X.F. Liu et al., Phys. Rev. Lett. **96**, 140604 (2006)
8. S. Sachdev, *Quantum phase transitions [M]* (John Wiley & Sons Ltd., Cambridge, England, 2007)
9. J. Zhang, X. Peng, N. Rajendran et al., Phys. Rev. Lett. **100**, 100501 (2008)
10. J. Zhang, F.M. Cucchietti, C.M. Chandrashekar et al., Phys. Rev. A **79**, 012305 (2009)
11. V. Jacques, P. Neumann, J. Beck et al., Phys. Rev. Lett. **102**, 057403 (2009)
12. A. Batalov, V. Jacques, F. Kaiser et al., Phys. Rev. Lett. **102**, 195506 (2009)
13. P. Pfeuty, Phys. Lett. A **72**, 245 (1979)
14. W. Liang, V.S. Ilchenko, A.A. Savchenkov et al., Optica **4**, 114 (2017)
15. T. Müller, M. Gilowski, M. Zaiser et al., Eur. Phys. J. D **53**, 273 (2009)